Parametrical evaluation of the aerodynamic performance of vertical axis wind turbines for the proposal of optimized designs

Andrés Meana-Fernández*, Irene Solís-Gallego, Jesús Manuel Fernández Oro, Katia María Argüelles Díaz, Sandra Velarde-Suárez

Fluid Mechanics Area, Department of Energy, University of Oviedo
C/Wifredo Ricart s/n Gijón Asturias 33204 Spain

Abstract

Many studies have tried to give insight into the optimal values of solidity and the airfoil geometry that maximize the performance and self-starting capability of vertical axis wind turbines, but there is still no consensus. In addition, most studies focus on one particular airfoil or airfoil family, which makes the generalization of the results difficult. In this work, these research gaps are intended to be assessed. An exhaustive analysis of the influence of solidity, blade Reynolds number and airfoil geometry on the performance of a straight-bladed vertical axis wind turbine has been performed using a methodology based on streamtube models. An airfoil database of 34 airfoils has been generated, developing a practical and cost-effective tool for the quick comparison of turbine designs (70 different configurations were analyzed). This tool, validated with results from the literature and computational fluid dynamics simulations performed by the authors, has allowed to propose an optimal solidity range from 0.25 to 0.5 and the use of almost symmetrical airfoils (camber $< 3\%$). Finally, this tool has been applied to design two vertical axis wind turbines optimized for low and medium wind speeds.

Keywords: VAWT design tool; streamtube models; airfoil data generation; CFD simulation

Nomenclature

α	Angle of attack
α_1	Upwind angle of attack
α_2	Downwind angle of attack

*Corresponding author: andresmf@uniovi.es

$\Delta\theta$ Size of vertical elements for the discretization of the rotor

ΔH Size of vertical elements for the discretization of the rotor

$\lambda = R\omega/V_\infty$ Turbine tip-speed ratio

μ Air dynamic viscosity

ω Turbine rotational speed

ρ Air density

$\sigma = Nc/R$ Turbine solidity

θ Angular blade position

c Blade chord

C_P Power coefficient of the turbine

C_{D_1} Upwind blade drag coefficient

C_{D_2} Downwind blade drag coefficient

C_{L_1} Upwind blade lift coefficient

C_{L_2} Downwind blade lift coefficient

C_{N_1} Upwind blade normal force coefficient

C_{N_2} Downwind blade normal force coefficient

C_{T_1} Upwind blade tangential force coefficient

C_{T_2} Downwind blade tangential force coefficient

CFD Computational Fluid Dynamics

D Drag force

$DDSM$ Double-disc streamtube model

$DMST$ Double-multiple streamtube model

f_{dw} Downwind actuator disk drag factor

f_{up} Upwind actuator disk drag factor

$HAWT$ Horizontal-axis wind turbine

L Lift force

$MSTM$ Multiple streamtubes model

N Force normal to the blade chord, number of blades

n	Number of actuator disks
N_s	Number of vertical elements for the discretization of the rotor
N_t	Number of azimuthal elements for the discretization of the rotor
P	Total power output of the turbine
p^+	Pressure before the actuator disk
p^-	Pressure after the actuator disk
P_1	Power of the turbine (upwind contribution)
P_2	Power of the turbine (downwind contribution)
p_∞	Ambient pressure
R	Turbine radius
$Re = \rho W c/\mu$	Blade Reynolds number
Re_1	Upwind blade Reynolds number
Re_2	Downwind blade Reynolds number
$SSTM$	Single streamtube model
T	Force tangential to the blade chord
T_1	Torque at the turbine (upwind contribution)
T_2	Torque at the turbine (downwind contribution)
T_{B_1}	Torque at a blade (upwind)
T_{B_2}	Torque at a blade (downwind)
T_{S_1}	Torque at a blade element (upwind)
T_{S_2}	Torque at a blade element (downwind)
u_1	Upwind induction factor
u_2	Downwind induction factor
V	Wind velocity at the turbine blades
V_1	Upwind induced velocity
V_2	Downwind induced velocity
V_∞	Freestream wind velocity
V_w	Wind velocity at the turbine wake

$VAWT$ Vertical-axis wind turbine

W Blade relative velocity

W_1 Upwind blade relative velocity

W_2 Downwind blade relative velocity

x Streamwise position

y Crosswise position

1. Introduction

In a world context focused on the reduction of greenhouse emissions, the development of renewable and sustainable energy sources is of vital importance. Wind energy is currently one of the most economical energy sources, as it employs a totally mature energy harvesting technology. In this scenario, small vertical axis wind turbines (VAWTs) are one of the best choices for direct energy generation, not only in remote locations but also in rural and urban areas. These turbines match perfectly the wind conditions of these areas, as they do not require high wind speeds and they can work independently of the wind direction. In addition, the noise level generated by this type of turbines is very low in comparison with horizontal axis wind turbines (HAWTs) and the installation and maintenance labors are much simpler, as the generator may be placed on the ground [1]. The main disadvantage of VAWTs, on the other hand, is their difficulty to self-start as a result of their particular aerodynamics [2].
At early design stages, many different rotor configurations must be compared before selecting a final design. Nevertheless, a straightforward design procedure is still lacking, fact that prevents several designs reported in the literature from achieving higher performances [3]. Two types of approaches have been used to predict the performance of VAWTs: Computational Fluid Dynamics (CFD) simulations and semiempirical methods such as momentum, vortex or cascade models [4]. Momentum models, such as streamtube models, despite being more robust and faster than CFD methods, require abundant experimental data for the airfoil lift and drag coefficients over a wide range of angles of attack and Reynolds numbers [5], [6]. CFD and experimental methods are very useful for the characterization of VAWTs [7], [8], [9], but streamtube models present themselves as the most convenient method for optimization exercises [10]. They are faster with regards to computational effort and time. Besides, previous studies by Balduzzi et al. [11] show that the results obtained with such models are in a qualitatively good agreement with CFD results. Different authors have also highlighted the importance of these models for the industrial environment, due to their extremely small computational requirements [12]. Bedon et al. [13] have also compared these models with experimental results, finding a good agreement and then using the models to optimize the shape of the blades of a Darrieus turbine. However, the formulation of streamtube models is complex enough that a

formula based numerical optimization process becomes difficult. Hence, most of optimization studies using these models are based on the one-factor-at-a-time approach, in which control parameters are modified separately and the optimum is determined from the combination of the results of the analysis.

The performance and self-starting capability of a VAWT depends on several parameters that relate to the whole turbine and flow conditions. Nevertheless, there are three parameters that have a major influence on the turbine performance: the turbine solidity, the flow Reynolds number and the airfoil used to fabricate the blades [14], [15]. Many studies have tried to give insight into the optimum values of these parameters, but the results seem contradictory.

Starting from a proposed optimal value for the solidity of 0.2 by [16] and [17], other authors propose ranges of values between 0.2 and 0.6 [3], 0.3 and 0.5 [18], or 0.4 and 0.8 [1], while others have found such dissimilar values as 1 [19], 0.93 [20] or 0.34 [21]. This disparity highlights that there is still no consensus on the optimal solidity for a VAWT. Jain and Abhishek [22] found an increase in the power coefficient with the increase of solidity, whereas Li et al. [23], [24] found exactly the opposite behavior. Subramanian et al. [25] verified that high solidity turbines performed better at low tip-speed ratios. As remarked by Ghasemian [26], some researchers recommend either high solidity values that increase the performance at lower tip-speed ratios, or low solidity values that increase the performance at higher tip-speed ratios with a wider operating range [27], [20], [1]. All these findings reveal that more insight into the optimum values of solidity is needed.

Regarding the airfoil chosen to build the turbine blades, there is even more controversy between symmetrical and unsymmetrical airfoils. Beri and Yao [28] state that symmetrical airfoils have minimum or negative torque generation at lower tip-speed ratios, but unsymmetrical blades show a reduced peak efficiency compared to conventional symmetrical airfoils. Bianchini et al. [29] also pose some doubts in the effective application of cambered blades due to their different behavior depending on the sign of the angle of attack. Chen and Kuo [30] state that the larger the camber of the blade, the better is the self-starting capability of the VAWT, and Sengupta et al. [15] have shown improved performance of cambered blades with respect to symmetrical blades. On the other hand, El-Samanoudy et al. [31] and Jafaryar et al. [32] claim that symmetrical or almost symmetrical airfoils perform better. Besides, as highlighted by Qamar and Janajreh [33], the literature does not show a comprehensive understanding of how solidity affects the performance of cambered VAWTs, especially with regard to the optimal configuration. These authors [34] found an improvement in the performance of VAWT at lower speeds using cambered blades. All the different results present in the literature suggest the need to obtain more insight into the influence of airfoil camber on the performance of VAWTs. Finally, most of the studies focus on the investigation of a particular airfoil or airfoil family and sometimes the proposal of variations on them. The reasons seem clear: the cost of the experimental design in the case of experimental studies, the time and computational costs required to perform CFD simulations of different airfoil geometries and, in the case of momentum models, the lack of airfoil data

available to introduce in the models [3], [12].
In this work, the research gaps previously mentioned are intended to be assessed. An exhaustive analysis of the influence of different variables (solidity, blade Reynolds number and airfoil geometry) on the performance of a straight-bladed VAWT has been performed using a methodology based on streamtube models. With the results obtained, insight into the optimum solidity for VAWTs and best airfoil characteristics is provided. The lack of available airfoil data for streamtube models is another research gap that is covered in this study, developing an airfoil database of 34 airfoils for VAWT applications at different angles of attack and Reynolds numbers. With the combination of this database and the streamtube models, a practical and cost-effective tool that allows the quick comparison of different turbine designs has been developed. This could help VAWT designers to propose different VAWT designs and predict their performance in computational times of the order of minutes. Finally, in order to illustrate the usefulness of this tool, two VAWT designs for low and medium wind speeds are proposed at the end of this paper.

2. VAWT aerodynamics and the self-starting problem

The flow developed through and around a VAWT is quite complex. When a VAWT starts rotating, the blades are positioned at a full range of angles of attack up to 180°. Besides, the blades in the upwind part, as well as the turbine tower, shed vortices that impinge on the downwind blades, affecting their performance. Figure 1 shows the top view of an H-rotor alongside the pressure and velocity evolution through the turbine as considered by the actuator disk theory [35]. The pressure increases from ambient pressure p_∞ up to a value of p^+ when reaching the turbine, then drops to p^- and finally recovers the value of the ambient pressure. The actual wind velocity that reaches the turbine is V, less than the ambient wind velocity V_∞. The turbine sheds a wake into the flow of an even lower velocity V_w. At the bottom of Figure 1, the velocity triangle and the aerodynamic forces on a particular blade position are shown. The angular blade position is denoted as θ. The rotational velocity of the blade is $R\omega$, being R the turbine radius and ω the rotational speed. The angle of attack α is the angle between the blade chord and the relative velocity. From these figures, it is clear that the flow and forces (drag - D, lift - L, normal - N, tangential, T) impinging on a blade are constantly changing during the rotor operation.
Defining the rotor solidity as $\sigma = Nc/R$, being N the number of blades and c the airfoil chord, the turbine tip-speed ratio as $\lambda = R\omega/V_\infty$ and the blade Reynolds number as $Re = \rho W c/\mu$, where W is the relative velocity, the power coefficient of the turbine may be expressed as:

$$C_P = f\{Re, \lambda, \sigma, airfoil\} \tag{1}$$

Hence, besides on the airfoil geometry, the performance of a VAWT depends mainly on the turbine Reynolds number, its tip-speed ratio and its solidity. The

characteristic curve of a VAWT is typically given in dimensionless terms, with the power coefficient as a function of the tip-speed ratio, as shown in Figure 2, where two typical VAWT power curves are depicted. When the turbine starts working from rest ($\lambda = 0$), it rotates only due to drag effects. Over time, it accelerates until its tangential velocity reaches the freestream wind velocity ($\lambda = 1$). After the turbine speed exceeds the freestream velocity, significant lift is produced on the turbine blades and it is considered that the starting process of the turbine has finished ($\lambda > 1$) [2].
For most VAWTs, there is a region of negative power coefficients at low tip-speed ratios that prevents the rotor from self-starting. The elimination of this region, the so-called dead band zone, is probably the main challenge for the definitive establishment of VAWT technology.

3. Methodology

3.1. Streamtube models

Streamtube models have been extensively described by Paraschivoiu [16]. They combine the actuator disk theory proposed by Glauert [35] iteratively with the blade element method in order to obtain the performance of a VAWT. The turbine is modeled as a theoretical disk that extracts energy from the wind due to the drag force exerted by the incoming flow. Firstly, the wind deceleration caused by the turbine/disk is supposed. Then, using the blade element method with this supposed velocity, the drag exerted by the wind on the turbine is calculated and compared with the disk drag. Eventually, once convergence is met, the wind velocity profiles, aerodynamic variables and the turbine performance may be calculated.
The first model, proposed by Templin [36], is the single streamtube model (SSTM). It considers a unique streamtube enclosing the whole turbine. Further developments consider multiple streamtubes instead (multiple streamtubes model (MSTM) [37]). Finally, the double-multiple streamtube model (DMST) considers two actuator disks to take into account the different conditions at the upwind and downwind parts of the turbine, each one with multiple streamtubes [16].
In this work, these 3 models have been implemented using a home-made MATLAB® code. In addition, a fourth model, the double-disc streamtube model (DDSM), with two actuator disks and just one streamtube, was developed as a simplification of the DMST model to test if a simplification of the model is sufficiently appropriate without a significant penalty in accuracy. The DMST model calculation scheme is displayed in Figure 3. As the rest of the models follow similar calculation schemes, they are not shown for the sake of brevity. The convergence criterion for the induction factors has been set to 10^{-6} and the maximum number of iterations has been set to 1000. With these criteria, the time required for the models to yield the complete C_P-λ curve of the VAWT is around five minutes. In the context of this work, a total of 70 different VAWT configurations were analyzed with this tool.

Momentum models present the disadvantage that the equations used under the disk approach are not applicable beyond high induction factors (0.5) [38]. In addition, some of them present convergence problems for low velocities (high induction factors or high λ), especially the ones with the double disk approach [16]. The breakdown problem of the momentum equation has been addressed via empirical correlations, which have widely enlarged the application range of these models (Glauert [35], Eggleston and Stoddard [39], Spera [40], Burton et al. [41], Manwell et al. [14], Buhl [38]). In this work, the Spera correction [40] has been applied for high induction factors. Despite these drawbacks, streamtube models are appropriate to reach the aim of this study, as they allow a quick comparison of different VAWT geometries during early design stages.
Before passing to the next section, a comment about the actuator disk theory and the Betz limit (16/27) must be made. This limit is the theoretical maximum power coefficient of a turbine modeled as one actuator disk, a well-known limitation in case of HAWT [14]. However, the actuator disk theory, as studied by Newman [42], may be extended to multiple actuator disks in tandem. Newman showed that the maximum power coefficient for a turbine modeled with n actuator disks is $8n(n+1)/[3(2n+1)^2]$. So, in the case of the a turbine modeled with two actuator disks (DDSM and DMST models), the maximum theoretical power coefficient is 16/25. Therefore, it is not surprising that VAWTs modeled with DDSM or DMST exceed C_P values of 0.6.

3.2. Generation of airfoil data

Streamtube models need values of the lift and drag coefficients of the airfoil as a function of the angle of attack and the blade Reynolds number. Experimental values would be desirable, but a literature survey highlights the difficulty of finding enough data, specially for high angles of attack and low Reynolds numbers. Aerodynamic data for seven symmetrical airfoils were generated by Sheldal and Klimas in 1981 [43], who performed wind tunnel test series for 4 NACA airfoils at Reynolds numbers of $0.35 \cdot 10^6$, $0.50 \cdot 10^6$ and $0.70 \cdot 10^6$. In order to extend the airfoil data to other airfoil sections as well as lower Reynolds numbers, they employed a synthesizer computer code, PROFILE [44]. However, some authors like Lazauskas used a minimum Reynolds number of 80,000 for their calculations [45], after considering the data from Sheldal and Klimas for lower Reynolds unusual and atypical. This such high variation of the aerodynamic data with the Reynolds number may be verified in the results from Bogateanu et al. [46], who show very different VAWTs performance curves depending on the Reynolds number. In addition to the uncertainty in the lift and drag values for different airfoils, it must not be forgotten that the angle of attack and Reynolds number are constantly changing during VAWT operation, so hysteresis effects in the lift and drag values arise.
However, the consideration of all these effects, besides other effects neglected by the model formulation (streamtube expansion, rotor tower and wake effects...) would mean a great increase of the calculation time, which is one of the constraints of this study. So, for the sake of developing a simple and practical model, XFOIL [47] has been used for generating the airfoil data. XFOIL has

a very good accuracy-computational cost ratio, and its viscous formulation has proven to be very useful for subcritical airfoil design, being particularly applicable to low Reynolds airfoils [47]. Nevertheless, it must be regarded that XFOIL predictions begin to fail past the airfoil stall angle. However, from a value of 30°, the airfoil geometry becomes unimportant and almost all airfoils behave as a flat plate [48]. This leaves a reduced region of uncertainty between the stall angle and 30°, which will affect the solution for particular blade positions. Anyway, this will only happen for a minimum part of the whole range of angles of attack found by the blade as it travels along the rotor, so this approach is still valid for the aim of this work.

The range of airfoil data needed for a particular application may be found from the definition of the angle of attack and blade Reynolds number. Before reaching $\lambda = 1$, the maximum angle of attack is always found at the position $\theta = \pi$ and decreases linearly from π at $\lambda = 0$ to $\pi/2$ at $\lambda = 1$. Once the turbine has passed $\lambda = 1$, the maximum angle of attack is found at the angular position:

$$\theta = acos\left(\frac{-u}{\lambda}\right) \tag{2}$$

The value of this maximum is, therefore:

$$\alpha = atan\left(\frac{\lambda usin\left[acos\left(\frac{-u}{\lambda}\right)\right]}{\lambda^2 - u^2}\right) \tag{3}$$

On the other hand, the maximum and minimum Reynolds numbers are always found at $\theta = 0$ and $\theta = \pi$, and their values are:

$$Re_{\theta=0} = \frac{\rho c V_\infty}{\mu}(\lambda + u) \tag{4}$$

$$Re_{\theta=\pi} = \frac{\rho c V_\infty}{\mu}(\lambda - u) \tag{5}$$

Setting $u = 1$ into the equations, the limits for the angles of attack and Reynolds numbers required for the analysis are obtained:

$$\alpha = atan\left(\frac{\lambda sin\left[acos\left(\frac{-1}{\lambda}\right)\right]}{\lambda^2 - 1}\right) \tag{6}$$

$$Re_{\theta=0,\pi} = \frac{\rho c V_\infty}{\mu}(\lambda \pm 1) \tag{7}$$

For this work, airfoil data have been generated for all angles of attack and the following Reynolds numbers: 10,000, 20,000, 40,000, 80,000, 160,000, 360,000, 700,000, 1,000,000, 2,000,000 and 5,000,000. The values for Reynolds numbers between the generated ones are obtained from linear interpolation. Table 1 contains a summary of typical 4-digit NACA airfoils that have been selected to obtain insight into the influence of thickness and camber in the performance of

a VAWT.
The generation of airfoil data has been extended to other airfoils specially designed for low-Reynolds applications. Firstly, the relatively new DU-06-W-200, an airfoil designed in Delft University [49] and that is allegedly supposed to present a good self-starting behavior. Another interesting airfoil is the NACA 0012H, a modification of the NACA 0012 employed for some Sandia VAWT tests [43]. The Wortmann FX-63-137 airfoil [50], based on the liver puffin wing, has been also analyzed. Finally, some Selig airfoils, S1020, S1012 and S8037, and two Natural-Laminar-Flow Airfoils, NLF0115 and NLF1015, have been studied as well [51]. The geometry of all these airfoils is presented in Figure 4.

3.3. Experimental validation

The results obtained with the four streamtube models have been compared with CFD and experimental results from Castelli et al. [7]. The turbine characteristics are collected in Table 2, and the results of the comparison are shown in Figure 5.
For low tip-speed ratios (lightly-loaded blades), the correspondence between the models and the experimental results is very good. However, at high tip-speed ratios (highly-loaded blades), the distribution of the velocities along the different azimuthal positions is particularly non-uniform. This explains the discrepancies between the models that employ just a streamtube (SSTM and DDSM) and the models that consider multiple streamtubes (MSTM and DMST)[16]. In addition, this turbine has a great solidity (around 0.5). For high solidities and high tip-speed ratios, the resolution of the momentum equation may break down, and the introduction or not of empirical correlations changes the results predicted by the models. Therefore, for actual design of turbines with high solidity and large tip-speed ratios, other predictive models (vortex models or CFD) would be more suitable.
Nevertheless, all of the developed models are able to follow the evolution of the C_P curve up to the maximum value and predict reasonably well the tip-speed ratio at which the maximum power coefficient is achieved (from the experimental results, it may be observed that this tip-speed ratio lays between 2.5 and 3). The predictions made by streamtube models match even better the experimental values than the CFD results, being the DMST model the most accurate.

3.4. CFD Numerical model

In order to increase the reliability of the proposed design methodology, a CFD simulation of a straight-bladed VAWT has been performed. As stated by Balduzzi et al [11], CFD tools are a source of data for improving the predictions of lower order models, which are key to industrial design due to their extremely small computational requirements. The geometrical characteristics of the simulated VAWT are summarized in Table 3.
The geometry and the mesh were generated with GAMBIT® and the Navier-Stokes equations that describe the fluid dynamics were solved with ANSYS FLUENT® using the k-ω-SST model for the closure of turbulence. The boundary conditions applied, as well as details of the generated mesh may be seen

in Figure 6. The domain is circular, with a velocity-inlet condition of 9 m/s and a pressure-outlet condition equal to atmospheric pressure. The extent of the domain (larger than 10 times the airfoil chord) is enough to ensure that the boundary conditions will not interfere in the flow developed inside the rotor. The sliding mesh technique has been applied, separating the domain in two subdomains. The interface between them has been placed as far from the rotor as possible, in order not to disturb the wake generated by the rotor. Finally, the wall boundary condition has been applied to the blades.

As found in [52], the commonly applied mesh refinement is computationally expensive and often not practical for a 2D VAWT model. Therefore, the mesh independence study has been performed following the criteria established by [53] and [54]. A numerical uncertainty of 1.6% in the C_P was obtained, with a total of 989,770 cells inside the fluid domain. The time step chosen for the simulations involved 1,440 time steps per rotor turn (0.25° per time step), which added a relative error of 0.2% to the numerical results.

The uncertainty of the numerical discretization was considered to be small enough, so the numerical results are suitable to validate the analytical models. Figure 7 shows a comparison between the results from the streamtube models and the CFD simulations. As it may be noticed, the disparities between the models are much lower than for the experimental case, in part due to the fact that the simulated turbine has less than half the solidity of the experimental turbine. In this case, the four models follow perfectly the tendency of the simulated values. It may be verified, nevertheless, that the double disk approach predicts with greater accuracy the tip-speed ratio at which the peak power coefficient is obtained.

In order to select one of the four models for the rest of the analysis, the evolution of the flow velocity with the streamwise position along the rotor was compared with the velocities predicted by each of the models. Figure 8 shows the results of this comparison. The most accurate model is clearly the DMST model, as the DDSM model underpredicts the velocities at the downstream part of the rotor. The SSTM and MSTM show good agreement with the simulation values; however, they provide no information about the evolution of the flow velocity as it passes across the rotor. The exact values of the velocity ratio (V/V_∞) for the CFD and streamtube models at $\lambda = 4$ may be found in Table 4.

To analyze the differences between the results of the four implemented models, the contours of vorticity are shown in Figure 9. As it may be appreciated, the vortices shed by the blades are carried in the streamwise direction, interacting with the blades and other vortices. Following the convention introduced in [55], the blade path may be divided in four different regions: upwind, downwind, windward and leeward. The flow behavior is clearly different between the upwind and downwind parts of the rotor, but there is also a significant difference between the windward and leeward regions, due to the relative movement of the blade with respect to the streamwise direction. Therefore, it is not surprising that the DMST model is the model which yields the most accurate results, as it accounts not only for the difference in the velocity deficit between the upwind and downwind parts but also between the different azimtuhal positions. Figure

10 shows the distribution of flow velocity along all the azimuthal positions of the VAWT rotor, comparing the results from the CFD simulations and the DMST model. Although some differences may be appreciated, the DMST model is capable of predicting the velocity distribution with high accuracy. Note that the peaks observed in the CFD results are a consequence of the passage of a blade at that particular time.
Finally, the forces on the blades have been monitored from the CFD simulations and compared with the results from the DMST model. Figure 11 shows the evolution of the stream and cross-streamwise forces as a function of the blade angular position for different tip-speed ratios. The DMST model reproduces the behavior obtained from the CFD simulations with great accuracy. The greatest discrepancies are found for the lowest tip-speed ratio ($\lambda = 2.5$), as a consequence of the wakes shed by the blades at this operating condition. However, even at this tip-speed ratio, the DMST model is capable of following the tendency of the CFD results, peaking at the same positions.
In conclusion, the DMST model has been proved to predict accurately the aerodynamic variables of interest for VAWT design: power coefficient as a function of the tip-speed ratio, evolution of the wind velocity as it crosses the rotor and forces exerted by the wind on the turbine blades. However, caution must be paid when using this model for high-rotor solidities and high tip-speed ratio values, as it might not reach convergence satisfactorily.

3.5. Comparison with other benchmarks

Before proceeding to the evaluation of the results of this work, the predictions of the developed model have been compared with results from other authors in order to increase the reliability of the model. A suitable benchmark has been generated with results from momentum models (Paraschivoiu et al. [56], Ahmadi et al.[3], Jain et al. [22]), CFD simulations (Bedon et al. [6], Gosselin et al. [17]) and experiments (Kjellin et al. [57], Eboibi et al. [21]). Figure 12 shows the comparison of the developed model with CFD benchmarks, whereas Figure 13 shows the comparison with experimental and momentum model benchmarks. There is a good agreement of the C_P values predicted for all the benchmarks compared. The deviations in the results may be ascribed to the simplicity of the developed model (no dynamic stall effects, strut losses, streamtube expansion, rotor tower and wake effects considered); however, it must be noticed that this model is capable of obtaining the whole $C_P - \lambda$ curve in a time of around five minutes. Hence, and considering the good ratio between the model accuracy and the computation time, the model is suitable for the purpose of this study: the analysis of the influencing variables on the performance of a VAWT in order to get insight into the optimum solidity and the best airfoil characteristics, in addition to developing a cost-effective tool that allows the quick comparison of different turbine designs.

4. Results

Once the model has been validated, it has been used to study the influence of the main parameters that affect the performance of a VAWT: the rotor solidity, the turbine Reynolds number and the airfoil geometry. The airfoil chosen to evaluate the influence of solidity and Reynolds number is the DU-06-W-200, for consistency with the previous section. Afterwards, different airfoil geometries have been evaluated with a constant value of solidity. Finally, the results of the study have been used to propose an optimized VAWT design.

4.1. Influence of solidity

Figure 14 shows the influence of solidity in the performance of a straight-bladed VAWT. As it may be observed, the power coefficient peaks at around a solidity of 0.5 and a tip-speed ratio of 2.7. It may be noticed as well that the band at which the power coefficient peaks becomes narrower with the increase of solidity. As the difference in the maximum power coefficient for the solidities of 0.5 and 1/3 is very small, the value of 1/3 has been chosen as the optimum solidity for the subsequent analyses. This value of solidity has a wider high-efficiency operating band and is less likely to cause breakdown of the resolution of the momentum equation in the DMST model and thus lead to inaccurate results. Regarding the maximum power coefficient values, it may seem shocking to have surpassed the Betz limit of 16/27. Nevertheless, as explained before, in the case of the DMST model, the maximum theoretical power coefficient is 16/25 [42], which explains why the results from these model may rise up to 0.64. An optimal solidity range may be established from 0.25 to 0.5, which is in agreement with the results from [18] and [21]. This analysis has allowed to reduce the extent of the optimal ranges proposed by [1] and [3], discarding solidity values higher than 0.5 as they only cause an increase in the turbine loading without increasing the power extracted from the air.

4.2. Influence of the blade Reynolds number

As the blade Reynolds number changes with the azimuthal position of the blade, the effect of this variable on the performance of the VAWT has been addressed studying its main contributors. For a given λ, there are two main parameters that affect the turbine blade Reynolds number: the freestream velocity and the turbine size. If the incoming freestream velocity is fixed, the rotor radius (size) determines the blade Reynolds numbers that will be found throughout the different blade positions, and vice versa.
Figure 15 (left) shows the influence of the incoming freestream velocity in the performance of a VAWT with a fixed radius. It may be noticed that there is a threshold velocity under which the VAWT is unable to generate power. This result agrees with the observed behavior in VAWTs [16], [58] and highlights the need of performing this kind of parametric study before proposing a VAWT design, as it will determine the cut-in wind speed of the turbine. As the freestream velocity increases, so does the blade Reynolds number and the power coefficient

of the turbine. However, from a certain velocity the rise is no longer appreciable and there is no further improvement in the performance of the VAWT. Furthermore, the forces on the blades become greater with no net result in the turbine performance, up to a point that might damage the turbine structure. For this reason, there is a cut-out wind speed to protect the structural integrity of the turbine. Finally, there is another observed effect that may be explained with help of Figure 15: the self-starting of some VAWTs after a sudden drop in the freestream velocity. Imagine a turbine that is unable to start working for steady wind conditions, rotating at a certain $\lambda_1 < 1$. If the wind velocity suddenly drops, the operating point of the turbine, which would continue rotating at the same speed for a while, may move to a region of a greater $\lambda_2 > 1$ and start producing power. Then, with the turbine already started, when the incoming wind velocity recovers, the turbine would increase its rotational speed to maintain λ_2', and the self-starting process would be finished.
The other parameter that determines the blade Reynolds number, when the incoming velocity is fixed, it the turbine radius (size). Figure 15 (right) shows the effect of rotor size in the performance of a VAWT for a constant turbine solidity. It may be appreciated that a greater radius implies greater Reynolds numbers for the same tip-speed ratio, which increase the performance of the VAWT. Therefore, a larger rotor will be more likely to self-start than a smaller one. For the case represented in this figure, a rotor radius lower than 0.25 would result in no power generation. This effect is really interesting, as it might help to discard certain turbine sizes before prototyping them. It may also explain why it is so difficult for certain small-scale models to self-start and generate power as a consequence of a wide dead band. Another idea that may be drawn from these results is the fact that, even though a small-scale model could be unable to generate power, that does not imply that a full-scale model with the same solidity and geometry will be unable to work efficiently.

4.3. Influence of the airfoil geometry

The airfoil geometry, as introduced before, is one of the most important contributors to the performance of a VAWT. Turbines of the same size and solidity with the same operating conditions may behave quite differently depending on the airfoil used to fabricate the blades. The main characteristics of a given airfoil geometry are its thickness and its camber. Therefore, a first analysis of a series of 4-digit NACA airfoils has been performed in order to obtain a general insight about the influence of these two airfoil characteristics.

4.3.1. Influence of thickness

Figure 16 shows the influence of the airfoil thickness in the performance of a VAWT with symmetrical NACA00xx blades. A thicker airfoil helps starting the turbine and reaching higher power outputs; however, past a certain point, increasing the thickness of the airfoil becomes detrimental to the VAWT performance. The explanation of this effect is the increase in the drag forces on the blade. Although these forces may help the turbine to start rotating, at nominal

speeds they reduce the amount of power captured from the wind. Hence, the most suitable choice would be an airfoil as thin as possible, but allowing for self-starting and the development of a wide high-efficiency band (between 15% and 21%). This result is in agreement with the results presented by [17], who found NACA 0015 to be optimal compared to thinner and thicker airfoils of the same family.

4.3.2. Influence of camber

Following, the effect of adding camber to a symmetrical NACA 00xx airfoil has been studied. Figure 17 shows the results of adding camber to a NACA 0018 airfoil in the performance of a VAWT. When camber is added to the airfoil, the upwind part of the turbine benefits from higher lift at smaller angles of attack. On the other hand, the performance of the blades at the downwind part becomes worse. In Figure 17, it may be appreciated that adding a small amount of camber to the blade enhances the performance of the turbine, as stated by [32]. Nevertheless, too much camber results in a worse performance of the turbine (for 6% camber the maximum power coefficient reached is below 0.5), confirming that unsymmetrical blades show a reduced peak efficiency compared to conventional symmetrical airfoils [28]. Therefore, from Figure 17 it may be deduced that the selection of the airfoil for a VAWT should lean towards symmetrical or low-cambered airfoils (camber less than 3%), as those will produce the highest power output (result similar to [34]). The use of greater camber values, however, would be justified for small VAWTs which otherwise would be unable to self-start (see the comments about the effect of the size of the turbine on its performance).

4.3.3. Airfoils for low Reynolds applications

Figure 18 shows the results of the analysis of different airfoils specially designed for low-Reynolds applications, with the aim of determining which would be suitable for a VAWT.

The Selig airfoils studied show quite different behaviors. First of all, the S1012 presents an excellent performance compared to the other two. It may be appreciated that the S1020, as a consequence of the higher camber, presents a steeper $C_P - \lambda$ curve, but peaks at a lower power coefficient. For the S8037, it may be seen that the addition of just a small amount of camber causes a better self-starting behavior than for the other two airfoils. In addition, the peak performance is not so low compared with the highest C_P of S1012. This airfoil, thus, might represent a good choice for small-scale VAWTs.

The Natural-Laminar-Flow airfoils show a bad behavior compared to the other airfoils. The NLF(1)-0115 has a broad high performance band which would be of interest to make easier the electronic regulation of the turbine, but it peaks at around 0.4. On the other hand, the high camber of the NLF1015 makes it unsuitable for VAWT operation.

From the last set of airfoils, the FX 63-137 is also unable to reach power coefficients higher than 0.37 due to its high camber. It must be considered, however, that this airfoil was designed for flight applications, so it was not conceived to work beyond stall and obviously not at the VAWT typical angles of attack [50].

The NACA 0012H and NACA 23016 show a very good behavior, and are excellent candidates for VAWT applications. Finally, the DU-06-W-200 is a very good example of airfoil optimization. Starting from a NACA 0018 airfoil and modifying slightly its geometry, this airfoil outperforms the rest of the studied airfoils. The addition of just a little camber enhances strongly the self-starting capability of this airfoil, while the peak efficiency is not heavily affected. Therefore, it would be the best choice among the rest of the airfoils studied in terms of performance.

4.4. Application of the model to a case study: VAWTs for low and medium wind speeds

Based on the results of this study, an optimized design for a VAWT turbine may be proposed, which would work following the $Cp - \lambda$ curve of the DU-06-W-200 airfoil. Considering a small-scale VAWT of 1.5 kW to work at a nominal speed of 9 m/s, the characteristics of the proposed design are collected on the left column of Table 5. Additionally, a design for lower wind speed conditions (4.5 m/s) has been proposed on the right column of the same table. This turbine, as it may be observed, requires a higher rotor radius in order to maintain the Reynolds numbers necessary to keep a high power coefficient.
Finally, a one-factor-at-a-time analysis was performed to study the sensitivity of the model with respect to the most influencing parameters: the freestream velocity V_∞, the turbine radius R and the blade chord c. The results highlighted that the maximum deviation in C_P is below 1.2% when varying these parameters between 90% and 110% of the values proposed.

5. Conclusions

Streamtube models have been confirmed as one of the most convenient methods for VAWT optimization exercises, with a high ratio between accuracy and computational costs. The performance of a VAWT depends on several variables, being the turbine solidity, the blade Reynolds number and the airfoil used to fabricate the blades the ones with a major influence. Many studies have tried to give insight into the optimum values of these parameters, but there is still no consensus neither on the optimal solidity for a VAWT nor on the geometry of the airfoil chosen for the blades. In addition, most of the studies focus on the investigation of only one particular airfoil or airfoil family, which makes the generalization of results difficult.
In this work, it has been intended to assess these research gaps. An exhaustive analysis of the influence of the turbine solidity, blade Reynolds number and airfoil geometry on the performance of a straight-bladed VAWT has been performed using a methodology based on streamtube models. Three streamtube models from the literature and a fourth based on the simplification of the most complex one have been implemented in MATLAB® with self-made codes. The lack of available airfoil data for streamtube models has been covered by generating a database of lift and drag coefficients for 34 airfoils. The combination

of this database and the programmed codes has resulted into a practical and cost-effective tool for the quick comparison of VAWT designs (computational times around five minutes to obtain the whole $\lambda - C_P$ curve). This tool has been validated with both experimental and numerical results from the literature. Besides, a numerical CFD simulation has been performed in order to obtain more information about the flow behavior around and across the turbine for further validation of the developed tool.

It was found that an increase in the turbine solidity up to 0.5 led to higher power coefficients, but at the expense of reducing the high-efficiency band of the turbine, as confirmed by other authors. Based on the results of this work, a more reduced range of optimal solidity values (0.25-0.5) is proposed. The influence of the blade Reynolds number, considered only in few studies, seems very important in this case, giving insight into VAWT self-starting and power generation. Regarding the airfoil used to fabricate the blades, it was found that the optimal airfoil should be as thin as possible, but allowing for self-starting and a wide high-efficiency band. The influence of camber was found to be detrimental up from a certain value, driving the recommendation of airfoil selection towards symmetrical or low-cambered airfoils (camber below 3%).

Finally, some airfoils specially designed for low-Reynolds applications were analyzed, finding that the DU-06-W-200, the S1012, the NACA0012H and the NACA 23016 behaved quite efficiently. To conclude this work and illustrate the potential of the developed tool for the proposal of optimized designs, it was applied to design two VAWTs for low (4.5 m/s) and medium (9 m/s) wind speeds.

Despite the good accuracy of the developed tool and its low computational cost, it seems unable to model VAWTs with very high solidities due to the breakdown of the momentum equation. In addition, the model formulation does not allow the characterization of the complete flow field around the VAWT, neglecting wake shedding from the rotor tower and blades. For this reason, future studies with numerical simulations and experimental tests of the proposed designs should be performed in order to obtain a better characterization of the flow field around the turbine. Nevertheless, this tool may still help VAWT designers to propose different VAWT designs and predict their performance in computational times of just minutes, fact that made possible the analysis of 70 different VAWT configurations within this work.

Acknowledgment

This work has been supported by the "FPU" predoctoral research scholarship provided by the Spanish Ministry of Education, Culture and Sports and the "Severo Ochoa" predoctoral research scholarship provided by the Principality of Asturias, Spain. The authors also want to acknowledge the support from the Projects "Desarrollo de una herramienta de diseño optimizado de perfiles aerodinámicos para su utilización en turbinas eólicas de eje vertical" from the University Institute of Industrial Technology of Asturias, financed by the City Council of Gijón, Spain and "Diseño optimizado de una turbina eólica de eje

vertical" from the University of Oviedo Foundation, financed by the company AST Ingeniería.

References

[1] M.H. Mohamed. Performance investigation of H-rotor Darrieus turbine with new airfoil shapes. *Energy*, 47:522–530, 2012.

[2] N. Hill, R. Dominy, G. Ingram, and J. Dominy. Darrieus turbines: the physics of self-starting. *Proceedings of the Institution of Mechanical Engineers, Part A: Journal of Power and Energy*, 223(1):21–9, 2009.

[3] M. Ahmadi-Baloutaki, R. Carriveau, and D.S.-K. Ting. Straight-bladed vertical axis wind turbine rotor design guide based on aerodynamic performance and loading analysis. *Proceedings of the Institution of Mechanical Engineers, Part A: Journal of Power and Energy*, 228:742–759, 2014.

[4] G. Bedon, U.S. Paulsen, H.A. Madsen, F. Bellonia, M.R. Castelli, and E. Benini. Aerodynamic Benchmarking of the Deepwind Design. *Energy Procedia*, 75:677–682, 2015.

[5] J. Chen, L. Chen, H. Xu, H. Yang, C. Ye, and D. Liu. Performance improvement of a vertical axis wind turbine by comprehensive assessment of an airfoil family. *Energy*, 114:318–331, 2016.

[6] G. Bedon, S. De Betta, and E. Benini. Performance-optimized airfoil for Darrieus wind turbines. *Renewable Energy*, 94:328–340, 2016.

[7] M.R. Castelli, A. Englaro, and E. Benini. The Darrieus wind turbine: Proposal for a few performance prediction model based on CFD. *Energy*, 36:4919–34, 2011.

[8] C.S. Ferreira, G. van Kuik, G. van Bussel, and F.Scarano. Visualization by PIV of dynamic stall on a vertical axis wind turbine. *Experiments in Fluids*, 46:97–108, 2009.

[9] S. Joo, H. Choi, and J. Lee. Aerodynamic characteristics of two-bladed H-Darrieus at various solidities and rotating speeds. *Energy*, 90:439–451, 2015.

[10] M. Abdul Akbar and V.Mustafa. A new approach for optimization of Vertical Axis Wind Turbines. *Journal of Wind Engineering and Industrial Aerodynamics*, 153:34–45, 2016.

[11] Francesco Balduzzi, Jernej Drofelnik, Alessandro Bianchini, Giovanni Ferrara, Lorenzo Ferrari, and Michele Sergio Campobasso. Darrieus wind turbine blade unsteady aerodynamics: a threedimensional Navier-Stokes CFD assessment. *Energy*, 128:550–563, 2017.

[12] J. Thé and H. Yu. A critical review on the simulations of wind turbine aerodynamics focusing on hybrid RANS-LES methods. *Energy*, 138:257–289, 2017.

[13] G. Bedon, M.R. Castelli, and E. Benini. Proposal for an innovative chord distribution in the Troposkien vertical axis wind turbine concept. *Energy*, 66:689–98, 2014.

[14] J.F. Manwell, J.G. McGowan, and A.L. Rogers. *Wind Energy Explained*. John Wiley & Sons Ltd., West Sussex, England, 2002.

[15] A.R. Sengupta, A. Biswas, and R. Gupta. Studies of some high solidity symmetrical and unsymmetrical blade H-Darrieus rotors with respect to starting characteristics, dynamic performances and flow physics in low wind streams. *Renewable Energy*, 93:536–547, 2016.

[16] I. Paraschivoiu. *Wind Turbine Design: With Emphasis on Darrieus Concept*. Presses internationales Polytechnique, Canada, 2002.

[17] R. Gosselin, G. Dumas, and M. Boudreau. Parametric study of H-Darrieus vertical-axis turbines using uRANS simulations. In *21st Annual Conference of the CFD Society of Canada*, pages 1–16, Sherbrooke, Canada, May 2013.

[18] P. Sabaeifard, H. Razzaghi, and A. Forouzandeh. Determination of Vertical Axis Wind Turbines Optimal Configuration through CFD Simulations. In *IPCBEE vol.28*, pages 109–113, Singapore, Feb 2012. IACSIT Press.

[19] M.A. Singh, A. Biswas, and R.D. Mishra. Investigation of self-starting and high rotor solidity on the performance of a three S1210 blade H-type Darrieus rotor. *Renewable Energy*, 76:381–387, 2015.

[20] D. Gang and W.C. Kau. Unsteady Flow Numerical Simulation of Vertical Axis Wind Turbine. *Procedia Engineering*, 99:734–740, 2015.

[21] O. Eboibi and L.A.M. Danaoand R.J. Howell. Experimental investigation of the influence of solidity on the performance and flow field aerodynamics of vertical axis wind turbines at low Reynolds numbers. *Renewable Energy*, 92:474–483, 2016.

[22] P. Jain and A. Abhishek. Performance prediction and fundamental understanding of small scale vertical axis wind turbine with variable amplitude blade pitching. *Renewable Energy*, 97:97–113, 2016.

[23] Q. Li, T. Maeda, Y. Kamada, J. Murata, K. Shimizu, T. Ogasawara, A. Nakai, and T. Kasuya. Effect of solidity on aerodynamic forces around straight-bladed vertical axis wind turbine by wind tunnel experiments (depending on number of blades). *Renewable Energy*, 96:928–939, 2016.

[24] Q. Li, T. Maeda, Y. Kamada, K. Shimizu, T. Ogasawara, A. Nakai, and T. Kasuya. Effect of rotor aspect ratio and solidity on a straight-bladed vertical axis wind turbine in three-dimensional analysis by the panel method. *Energy*, 121:1–9, 2017.

[25] A. Subramanian, S.A. Yogesh, H. Sivanandan, A. Giri, M. Vasudevan, V. Mugundhan, and R.K. Velamati. Effect of airfoil and solidity on performance of small scale vertical axis wind turbine using three dimensional CFD model. *Energy*, 133:179–190, 2017.

[26] M. Ghasemian and Z.N. Ashrafiand A. Sedaghat. A review on computational fluid dynamic simulation techniques for Darrieus vertical axis wind turbines. *Energy Conversion and Management*, 149:87–100, 2017.

[27] Y.-T. Lee and H.-C. Lim. Numerical study of the aerodynamic performance of a 500 W Darrieus-type vertical-axis wind turbine. *Renewable Energy*, 83:407–415, 2015.

[28] H. Beri and Y. Yao. Effect of camber airfoil on self starting of a vertical axis wind turbine. *Journal of Environmental Science and Technology*, 4:302–312, 2011.

[29] A. Bianchini, G. Ferrara, and L. Ferrari. Design guidelines for H-Darrieus wind turbines: Optimization of the annual energy yield. *Energy Conversion and Management*, 89:690–707, 2015.

[30] C.-C. Chen and C.-H. Kuo. Effects of pitch angle and blade camber on flow characteristics and performance of small-size Darrieus VAWT. *Journal of Visualization*, 16:65–74, 2013.

[31] M. El-Samanoudy, A.A.E. Ghorab, and Sh.Z. Youssef. Effect of some design parameters on the performance of a Giromill vertical axis wind turbine. *Ain Shams Engineering Journal*, 1:85–95, 2010.

[32] M. Jafaryar, R. Kamrani, M. Gorji-Bandpy, M. Hatami, and D.D. Ganji. Numerical optimization of the asymmetric blades mounted on a vertical axis cross-flow wind turbine. *International Communications in Heat and Mass Transfer*, 70:93–104, 2016.

[33] S.B. Qamar and I. Janajreh. A comprehensive analysis of solidity for cambered darrieus VAWTs. *International Journal of Hydrogen Energy*, 42:19420–19431, 2017.

[34] S.B. Qamar and I. Janajreh. A comprehensive analysis of solidity for cambered darrieus VAWTs. *Energy Procedia*, 105:537–543, 2017.

[35] H. Glauert. *The Elements of Aerofoil and Airscrew Theory*. Cambridge University Press, Canada, 2 edition, 1947.

[36] R.J. Templin. Aerodynamic Performance Theory for the NRC Vertical-Axis Wind Turbine. Technical report, N.A.E. Report LTR-LA-160, 1974.

[37] J.H. Strickland. The Darrieus Turbine: A Performance Prediction Model Using Multiple Streamtube. Technical report, Sandia Laboratories Report SAND75-0431, 1974.

[38] M.L. Jr. Buhl. A new empirical relationship between thrust coefficient and induction factor for the turbulent windmill state. Technical report, National Renewable Energy Laboratory, Golden, Colorado, USA, 2005.

[39] D.M. Eggleston and F.S. Stoddard. *Wind turbine Engineering Design*. Van Nostrand Reinhold, New York, NY, USA, 1987.

[40] D.A. Spera. *Wind Turbine Technology*. ASME Press, New York, USA, 1994.

[41] T. Burton, D. Sharpe, N. Jenkins, and E. Bossanyi. *Wind Energy Handbook*. John Wiley & Sons Ltd., West Sussex, England, 2011.

[42] B.G. Newman. Multiple actuator-disk theory for wind turbines. *Journal of Wind Engineering and Industrial Aerodynamics*, 24:215–225, 1986.

[43] R.E. Sheldal and P.C. Klimas. Aerodynamic Characteristics of Seven Symmetrical Airfoil Sections Through 180-Degree Angle of Attack for Use in Aerodynamic Analysis of Vertical Axis Wind Turbines, Tech. Rep. SAND80-2114. Technical report, Sandia National Laboratories, Albuquerque, NM, USA, 1981.

[44] R. Eppler. Turbulent airfoils for general aviation. *Journal of Aircraft*, 15:93–99, 1978.

[45] L. Lazauskas. Three pitch control systems for vertical axis wind turbines compared. *Wind Engineering*, 16(5):269–282, 1992.

[46] R. Bogateanu, A. Dumitrache, H. Dumitrescu, and C.I. Stoica. Reynolds Number Effects on the Aerodynamic Performance of Small VAWTs. *U.P.B. Sci. Bull., Series D*, 76(1):25–36, 2014.

[47] M. Drela. Xfoil: An analysis and design system for low reynolds number airfoils. In *Proceedings of the Conference Notre Dame*, pages 1–12, Indiana, USA, Jun 1989. Springer-Verlag Berlin Heidelberg.

[48] J.F. Manwell, J.G. McGowan, and A.L. Rogers. *Wind Energy Explained: Theory, Design and Application*. John Wiley and Sons, Ltd, Chichester, UK, 2009.

[49] M.C. Claessens. The Design and Testing of Airfoils for Application in Small Vertical Axis Wind Turbines. Master's thesis, November 2006.

[50] D. Althaus and F.X. Wortmann. *Stuttgarter Profilkatalog 1: Messergergebnisse aus dem Laminarwindkanal des Instituts fur Aerodynamik und Gasdynamik der Universitat Stuttgart*. Vieweg Verlag, Braunschweig, Wiesbaden, Germany, 1981.

[51] *UIUC Airfoil Data Site*, (accessed March 27, 2017). `http://m-selig.ae.illinois.edu/ads/coord_database.html`.

[52] K.M. Almohammadi, D.B. Ingham, L. Maa, and M. Pourkashan. Computational fluid dynamics (CFD) mesh independency techniques for a straight blade vertical axis wind turbine. *Energy*, 58:483–93, 2013.

[53] P.J. Roache. Quantification of uncertainty in computational fluid dynamics. *Annual Review of Fluid Mechanics*, 29(1):123–60, 1997.

[54] F. Stern, W.V. Wilson, H.W. Coleman, and E.G. Paterson. Comprehensive Approach to Verification and Validation of CFD Simulations - Part 1: Methodology and Procedures. *Journal of Fluids Engineering*, 123:793–802, 2001.

[55] G. Tescione, D. Ragni, C. He, C.J.S Ferreira, and G.J.W. van Bussel. Near wake flow analysis of a vertical axis wind turbine by stereoscopic particle image velocimetry. *Renewable Energy*, 70:47–61, 2014.

[56] I. Paraschivoiu, O. Trifu, and F. Saeed. H-Darrieus wind turbine with blade pitch control. *International Journal of Rotating Machinery*, 2009:1–7, 2009.

[57] J. Kjellin, F. Bulow, S. Eriksson, P. Deglaire, M. Leijon, and H. Bernhoff. Power coefficient measurement on a 12 kw straight bladed vertical axis wind turbine. *Renewable Energy*, 36:3050–3053, 2011.

[58] M.D. Bausas and L.A.M. Danao. The aerodynamics of a camber-bladed vertical axis wind turbine in unsteady wind. *Energy*, 93:1155–64, 2015.

Tables and figures

Table 1: Families of 4-digit NACA airfoils considered for the study

	Camber				
Thickness	0%c	2%c	4%c	6%c	8%c
12%c	NACA 0012	NACA 2412	NACA 4412	NACA 6412	NACA 8412
15%c	NACA 0015	NACA 2415	NACA 4415	NACA 6415	NACA 8415
18%c	NACA 0018	NACA 2418	NACA 4418	NACA 6418	NACA 8418
21%c	NACA 0021	NACA 2421	NACA 4421	NACA 6421	NACA 8421
25%c	NACA 0025	NACA 2425	NACA 4425	NACA 6425	NACA 8425

Table 2: Geometrical characteristics of the VAWT from Castelli et al.[7]

Number of blades N	3
Rotor radius R	0.515 m
Rotor height H	1.45 m
Blade chord c	85.8 mm
Rotor solidity σ	0.5
Airfoil	NACA 0021
Tip-speed ratio λ	0 to 4

Table 3: Geometrical characteristics of the simulated VAWT

Number of blades N	3
Rotor radius R	0.5 m
Rotor height H	1 (2D)
Blade chord c	40 mm
Rotor solidity σ	0.24
Airfoil	DU-06-W-200
Tip-speed ratio λ	0 to 6

Table 4: Non-dimensional throughflow velocity along the streamwise coordinate of the rotor for $\lambda = 4$

Position	$y = R$	$y = R/2$	$y = 0$	$y = -R/2$	$y = -R$
CFD	0.8896	0.8232	0.7438	0.6675	0.6219
SSTM			0.6568		
MSTM			0.6863		
DDSM		0.8307		0.5048	
DMST		0.8354		0.6330	

Table 5: Characteristics of the proposed VAWT designs

Wind speed	Medium	Low
Number of blades N	3	3
Rotor radius R	1 m	3 m
Rotor height H	3 m	5 m
Blade chord c	111 mm	333 mm
Rotor solidity σ	1/3	1/3
Airfoil	DU-06-W-200	DU-06-W-200
Nominal wind speed	9 m/s	4.5 m/s
Rated power	1.5 kW	1 kW
Maximum power coefficient	0.5798	0.5996

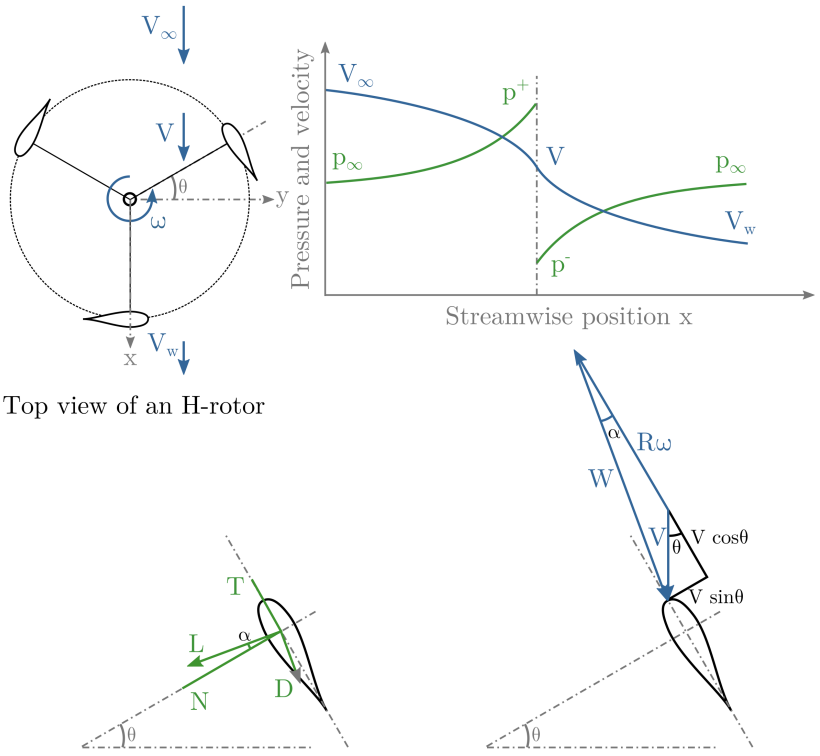

Figure 1: Aerodynamics of a VAWT rotor

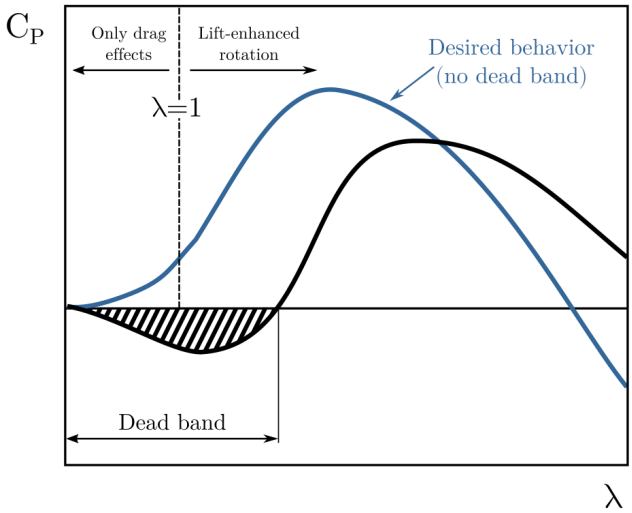

Figure 2: Typical power curves with dead band zones

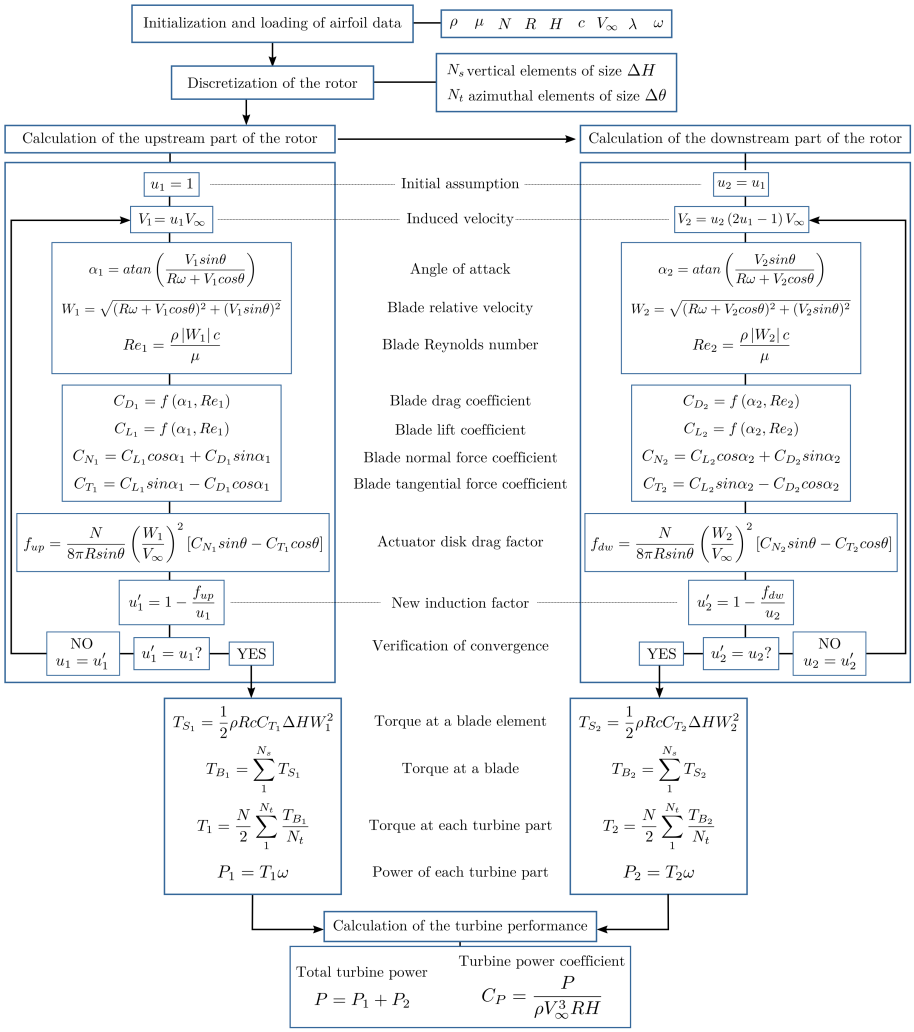

Figure 3: Calculation scheme of DMST model

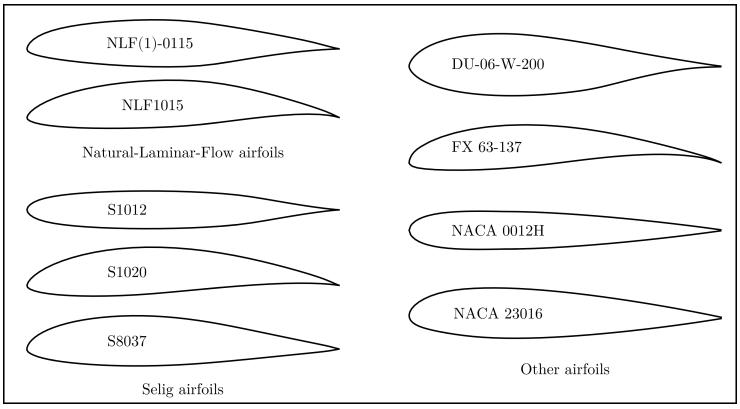

Figure 4: Typical airfoils for low-Re applications included in the study

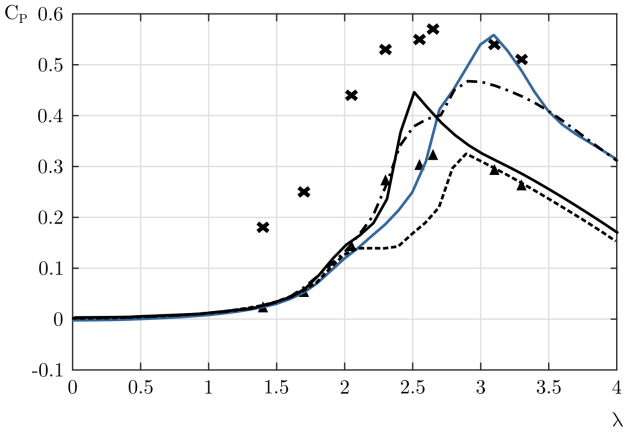

Figure 5: Comparison of streamtube models (SSTM-black line, MSTM-dashed line, DDSM-dash-dot line, DMST-blue line) with CFD (crosses) and experimental (triangles) results from Castelli et al.[7]

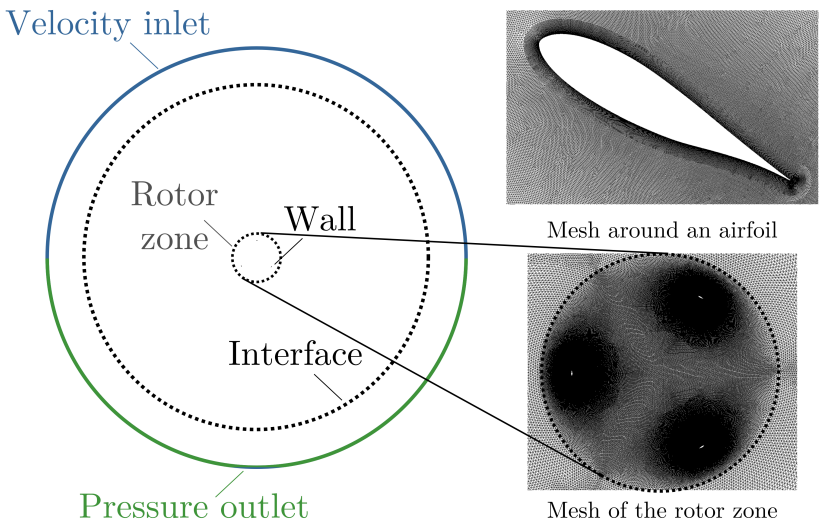

Figure 6: Computational domain with the boundary conditions applied. Mesh of the rotor domain and airfoil.

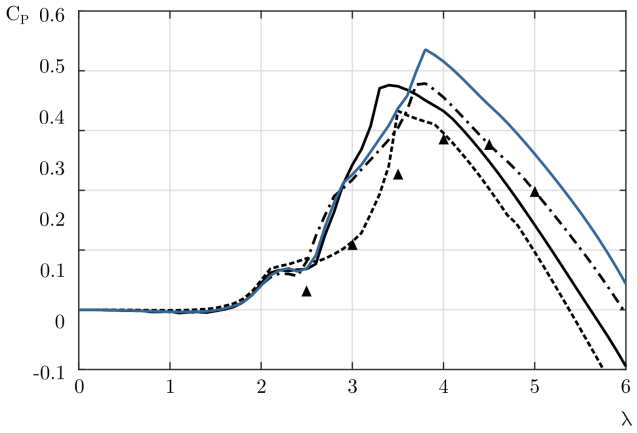

Figure 7: Comparison of streamtube models(SSTM-black line, MSTM-dashed line, DDSM-dash-dot line, DMST-blue line) with CFD results (triangles)

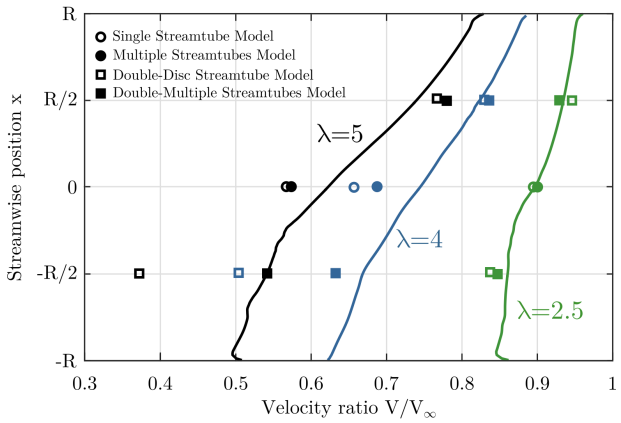

Figure 8: Evolution of the flow velocity along the turbine rotor

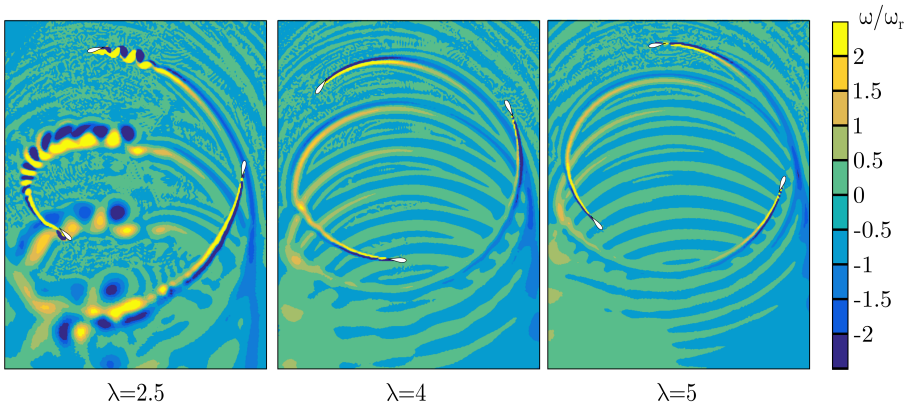

Figure 9: Contours of normalized vorticity in the fluid domain close to the VAWT rotor for three tip-speed ratio values

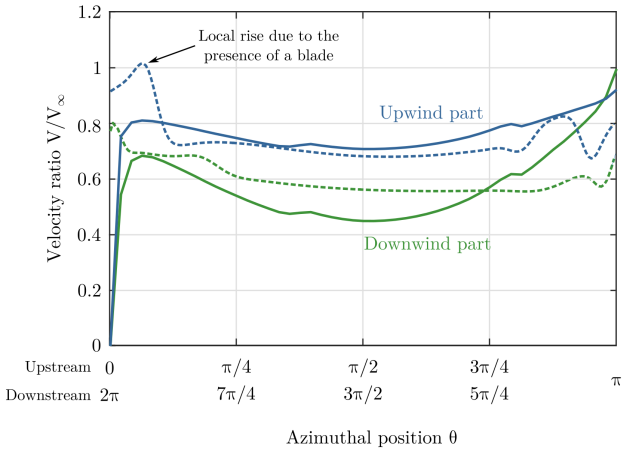

Figure 10: Velocity ratio along the rotor azimuthal positions (DMST model - solid lines, CFD - dashed lines)

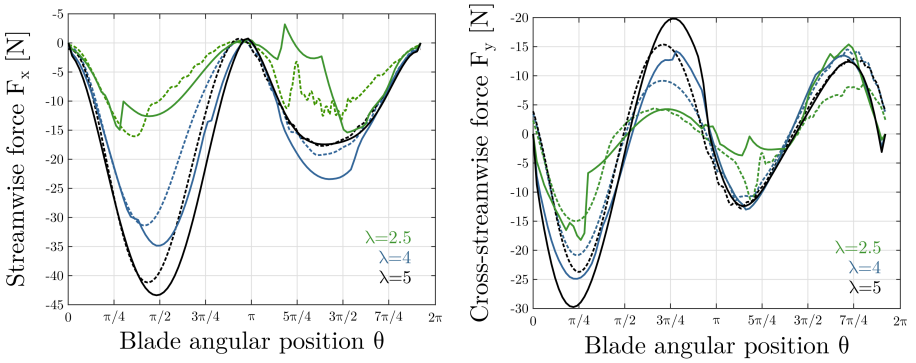

Figure 11: Stream and cross-streamwise forces on the blades for different tip-speed ratio values (DMST model - solid lines, CFD - dashed lines)

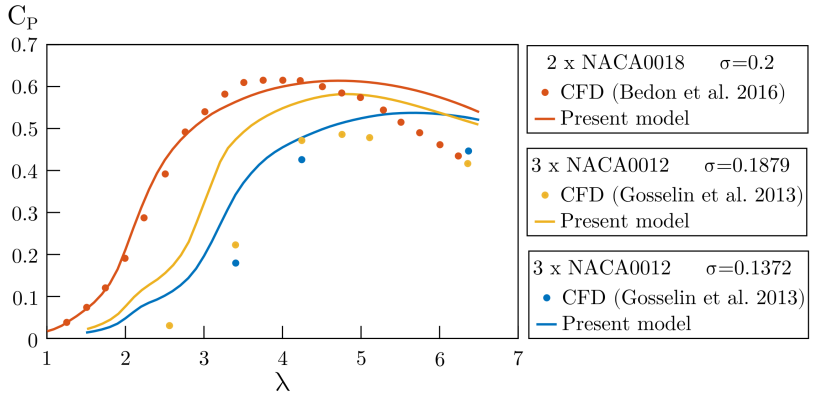

Figure 12: Comparison of the developed model with CFD benchmarks

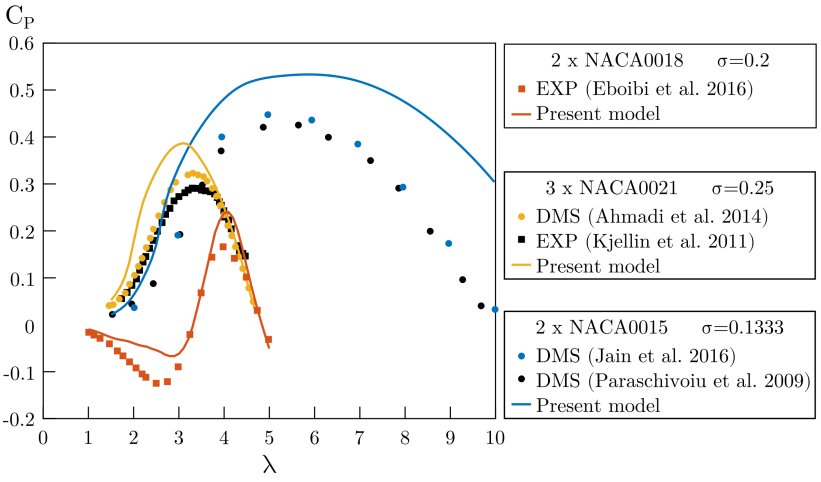

Figure 13: Comparison of the developed model with momentum model and experimental benchmarks

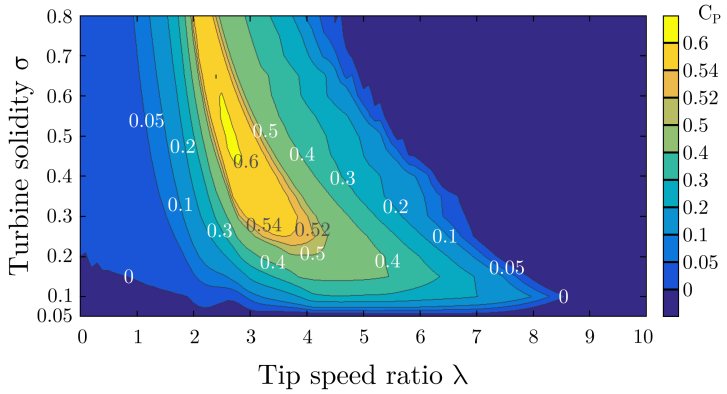

Figure 14: Influence of solidity in the performance of a VAWT

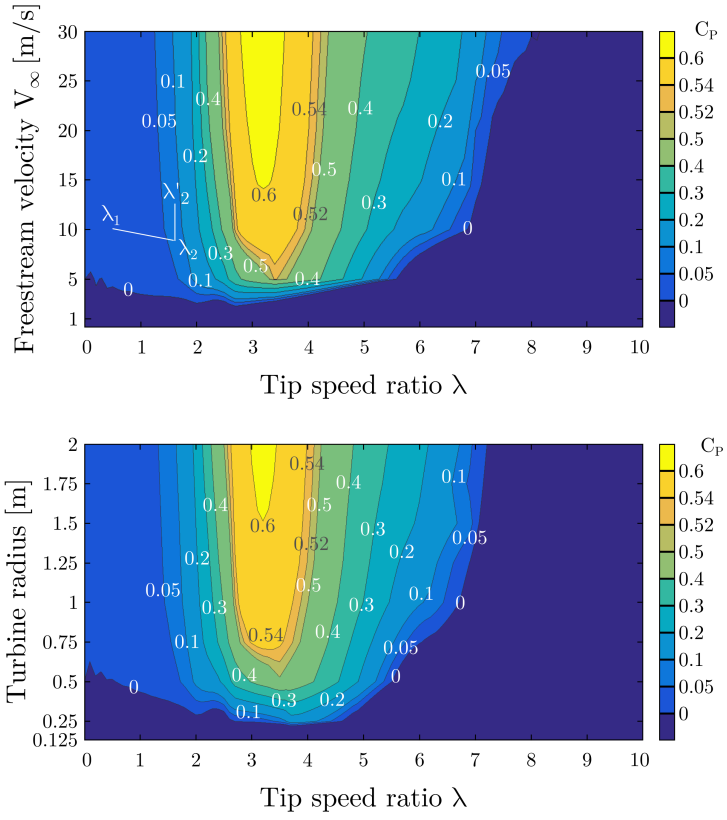

Figure 15: Influence of the freestream velocity and turbine radius (size) in the performance of a VAWT

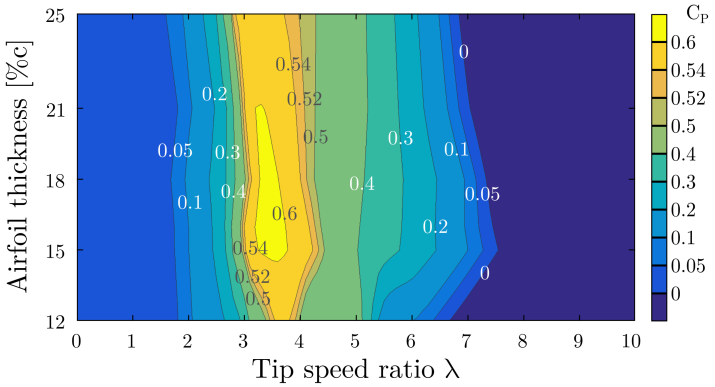

Figure 16: Influence of airfoil thickness in the performance of a VAWT with NACA blades

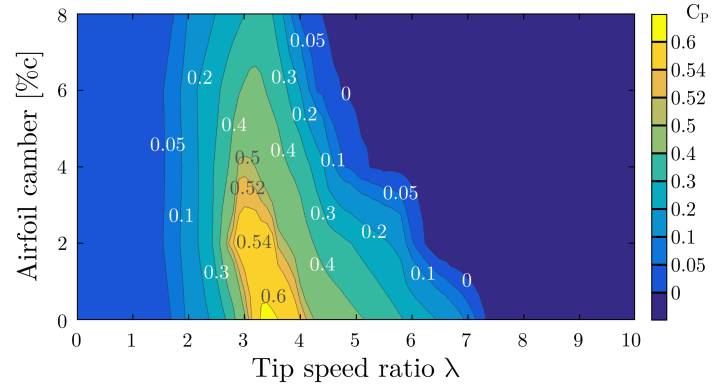

Figure 17: Influence of airfoil camber in the performance of a VAWT with NACA blades

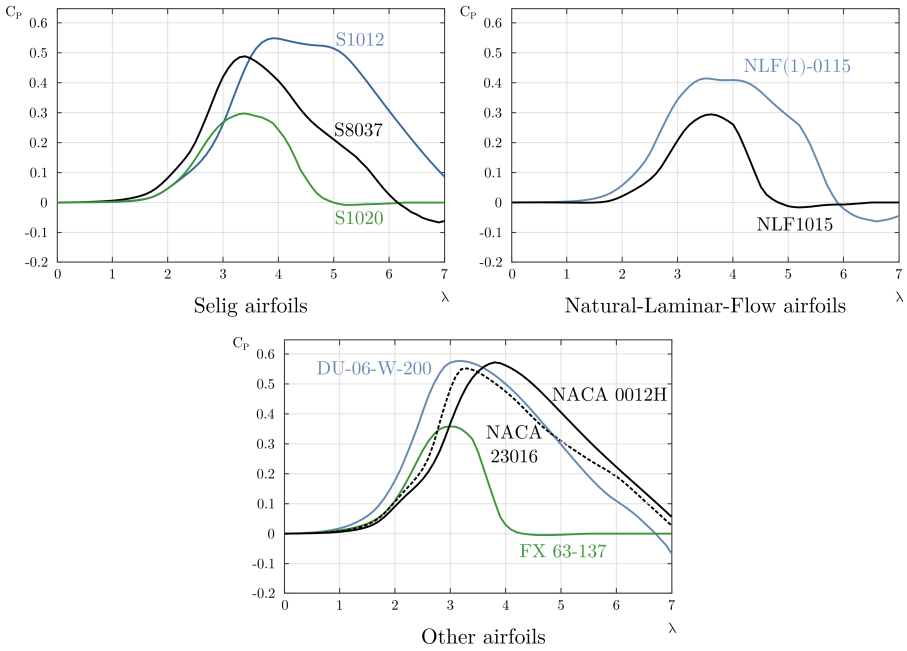

Figure 18: Performance curves of a VAWT with different airfoil concepts